Elsevier Editorial System(tm) for Journal of Alloys and Compounds
Manuscript Draft

Manuscript Number: JALCOM-D-08-02412R1

Title: Influence of processing route and reinforcement content on the creep fracture parameters of aluminium alloy metal matrix composites

Article Type: Normal Paper

Keywords: A. metals; B. powder metallurgy; D. high temperature alloys; D. creep.

Corresponding Author: Dr. Gaspar González-Doncel, PhD

Corresponding Author's Institution: CENIM, C.S.I.C.

First Author: Ricardo Fernández, PhD

Order of Authors: Ricardo Fernández, PhD; Gaspar González-Doncel, PhD

Abstract: An attempt to understand the rupture creep behavior of aluminum alloy metal matrix composites is made. Data from published investigations on the creep fracture of a variety of materials as well as new data on 6061Al-40vol%SiCw composite have been analyzed. The analysis is made on the basis of previous studies conducted by these authors in which the relevance of the load partitioning phenomenon was manifested. The well known phenomenological approach described by the Monkman-Grant equation has been employed. It is seen that the commonly used approximation of n´=1 (with n´ the Monkman-Grant exponent) is never satisfied. Rather, n´<1 is always obtained. A new form of this equation is proposed in order to understand the creep rupture mechanisms of these materials in greater depth.

* Manuscript plus Figures and Table
Click here to view linked References

# Influence of processing route and reinforcement content on the creep fracture parameters of aluminium alloy metal matrix composites

Ricardo Fernández[§] and Gaspar González-Doncel*

Dept. of Physical Metallurgy, Centro Nacional de Investigaciones Metalúrgicas (CENIM), C.S.I.C., Av. de Gregorio del Amo 8, E-28040 Madrid, Spain

[§] Present address, Thin Film R&D Dept. INDO, SA, C/ Alcalde Barnils 72, 08174 Sant Cugat del Vallés, Barcelona, Spain

## Abstract

An attempt to understand the rupture creep behavior of aluminum alloy metal matrix composites is made. Data from published investigations on the creep fracture of a variety of materials as well as new data on 6061Al-40vol%$SiC_w$ composite have been analyzed. The analysis is made on the basis of previous studies conducted by these authors in which the relevance of the load partitioning phenomenon was manifested. The well known phenomenological approach described by the Monkman-Grant equation has been employed. It is seen that the commonly used approximation of $n'=1$ (with $n'$ the Monkman-Grant exponent) is never satisfied. Rather, $n'<1$ is always obtained. A new form of this equation is proposed in order to understand the creep rupture mechanisms of these materials in greater depth.

*Key words:* A. metals; B. powder metallurgy; D. high temperature alloys; D. creep.

*** Corresponding author:** ggd@cenim.csic.es

## Introduction

The creep behavior of discontinuously reinforced metal matrix composites, MMCs, has been extensively studied [1-12]. The interest in these materials resides in their improved behavior with respect to their corresponding monolithic alloys. Furthermore, they can be produced at reasonable cost on a large scale, taking advantage of conventional procedures such as powder metallurgy, PM, or ingot metallurgy, IM, [13]. Recently, these authors [12] have shown the relevance of the load transfer mechanism during high temperature deformation as dominant strengthening mechanisms in these composites. In their work, Fernández and González-Doncel [12] conducted a comparative study of the creep behavior of a PM 6061Al-15vol%$SiC_w$ composite relative to the un-reinforced PM 6061Al alloy. They showed separately the role of, A) the dispersion of the aluminum oxide particles (nano-scale) introduced by the PM route and B) the ceramic particles (micro-scale) purposely introduced to enhance the creep properties of monolithic aluminum alloys. Furthermore, a microstructural factor associated with the shorter inter-obstacle distance for dislocation motion in the composite matrix was also considered. These findings were assessed by a thorough analysis of data recorded from the open literature. From this latest analysis, the influence of damage phenomena associated with the metal-ceramic interface was also estimated. Interfacial damage decreases the effectiveness of load transfer and composite creep strength is reduced. It could be deduced that IM composites are more inclined to develop damage mechanisms than materials obtained by the PM route [12]. The above finding is supported by the fact that IM composites are more prone to develop undesirable reaction products formed at the interface during melting of the metallic matrix than PM ones.

More recently [14], the importance of the load transfer mechanism was also revealed from the analysis of the time to rupture data in the framework of the Monkman-Grant, MG, and the Larson-Miller approaches [15,16]. The MG equation, in particular, is of great help for predicting the creep life of engineering components because of its simplicity. It extrapolates the data obtained from laboratory creep tests (which range from some few hours up to several months) to the real service conditions of components. In real life, these components operate during time periods which may well exceed several decades. The importance of the MG equation resides on the fact that it is obeyed by most engineering materials. In is original and general form this equation reads:

$$t_f \dot{\varepsilon}_{\min}^{n'} = C \quad (1)$$

Where $t_f$ is the time for creep rupture, $\dot{\varepsilon}_{\min}$th e minimum or steady strain rate, and $n'$ and $C$ are constants. $C$ is known as the Monkman-Grant constant, and would represent the total elongation to failure in case that $n'=1$ and $\dot{\varepsilon}_{\min}$ dominates the creep test. Usually, the value of the MG exponent, $n'$, is close to $n'=1$. For this reason a simplified version of equation 1, namely, $t_f \dot{\varepsilon}_{\min} = \varepsilon^*$ (where $\varepsilon^*$ has units of strain) is frequently used [11,17-20]. Under this restriction, it is agreed that this empirical equation reveals that creep strain is the macroscopic manifestation of the damage accumulated during deformation and that the fracture mechanisms are associated with the deformation mechanisms. A deviation of $n'$ from the "ideal" value of $n'=1$ "disturbs", somewhat, a rational interpretation of time to rupture data in the context of microstructural parameters and deformation mechanisms. In fact, the attempts to understand the MG equation in terms of deformation mechanisms and microstructural parameters have always been made on the basis that $n'=1$ [17,19].

Hence, the purpose of this work is to analyze further the creep rupture data of discontinuously reinforced metal matrix (aluminum alloy) composites and their respective un-reinforced alloys in the context of the MG equation with two objectives:

a) to understand better the specific role played by the ceramic particles in the creep rupture behavior of MMCs and,
b) to go further in the underlying basis of the MG equation.

Data recorded from the open literature as well as new data from a 6061Al-40vol%%$SiC_w$ composite will be analyzed.

**Time to creep rupture data**

Data from the open literature has been analyzed for this investigation [14,21-29]. Whenever possible, time to rupture data of aluminium alloy metal matrix composites and the corresponding un-reinforced alloys has been selected. Data of un-reinforced alloys and composite materials (without corresponding un-reinforced alloy data), has been also included. All the information is summarized in Table I. The materials investigated, the processing route (PM *vs*. IM materials, where IM also includes materials prepared by other routes, but different from PM), the creep conditions (stress and temperature of testing) as well as the MG parameters, $n'$ and $C$ constants, are reported in each case. Finally, the information regarding the possible improved (or

worsened) composite creep strength with respect to the corresponding un-reinforced alloy and microstructural data has been also considered in Table I.

**Material investigated and experimental part**

In addition to the above data review, new creep tests to failure have also been conducted on 6061Al-40vol%$SiC_w$ composite prepared by a proprietary PM procedure. The material was kindly supplied in the form of an extruded bar of 46 mm in diameter by Dr. J. Wolfenstine. Tensile creep specimens were machined with the tensile direction parallel to the extrusion axis direction. The gauge length was a cylinder, 10 mm in gauge length and 3 mm in diameter. Samples were threaded at the heads. Creep tests were conducted at 723 and 673 K and stress in the interval of 23-73 MPa using the same equipment described in [12]. Scanning and optical microscopy was used to study the microstructure.

**Results and discussion: Data analysis**

The creep rupture time data of the materials of Table I are shown in figures 1 and 2. Figure 1 corresponds to the PM materials [14,21,22,29] and figure 2 to the IM materials and the remaining materials, not processed by PM [15,23-28]. Data of PM 6061Al alloy and 6061Al-15vol%$SiC_w$ composite studied in [14] are represented only by the average line trend of data for the sake of simplicity. A common general trend is obtained in both figures. In all cases the MG relation is obeyed, but none of the materials presents a MG exponent equal to $n'=1$. As a general rule, PM materials reveal MG exponent values more grouped than IM materials ($n'$ ranges in the intervals 0.6-0.98 and 0.33-1.0 for the PM and IM materials, respectively). Although somewhat speculative, this result could be associated with "extra" accumulation of non-diffusion controlled interfacial damage. Such a process occurs, preferably, in IM composite materials [12,28]. As mentioned before, extra damage in these composites can be related to the undesirable reaction products formed in the liquid phase during material processing. Then, it is possible that the extra damage accumulates at a different rate with creep strain, depending on the applied stress (or strain rate, according to the power law behavior), resulting in a MG exponent, different from 1. In fact, being $n'<1$, as observed in most materials, Table I. This assumption does not undermine the idea that MG relation can be obeyed despite non-diffusion controlled damage occurs. Damage evolution would depend, also, on materials microstructure besides testing conditions.

On the other hand, the IM composites of ref. [28], with $n'$ values very different from unity, show only a slight improvement of the creep behavior with respect to un-reinforced A359 alloy. These results reveal that the improved creep response of the materials analyzed is not related to the MG exponent.

It has been found, however, that composite creep strengthening, as measured experimentally from the creep strain rate - stress plot of composite and un-reinforced alloy [12], is revealed in MG plots as a decrease in $t_f$ for any given strain rate or as a decrease in the strain rate for any given time to rupture (displacement towards the left of un-reinforced alloy data in MG plot). This trend was previously found in [14] and has also been assessed here for materials reported in [22,29] and for the present 6061Al-40vol%$SiC_w$ composite, figures 3a) and 3b) These figures are double logarithmic plots of the strain rate as a function of the stress in which the creep data of this composite appear together with that of 6061Al-15vol%$SiC_w$ composite and 6061Al alloy of refs. [12,14]. Figure 3a) reports the behavior at 673 and figure 3b) at 723 K. The increase in composite creep strength with reinforcement content can be seen. In parallel, $t_f$ of the composite, at any given strain rate, decreases with increasing the reinforcement content, figure 1. The microstructure of the 6061Al-40vol%$SiC_w$ composite is revealed in the micrograph of figure 4. As can be seen a homogeneous distribution of the high volume fraction of reinforcement has been obtained through PM. On the other hand, it has been reported that the creep response of the composite 2124Al-15vol% of ref. [21] is worse than that of the corresponding un-reinforced 2124Al alloy. In this case, however, the time to rupture of the composite is larger than that of the alloy at any given strain rate, figure 1, *i.e.*, the composite data in MG plot is located on the right of the alloy data.

A possible explanation for the above correlations is that materials failure is, indeed, the result of microscopic damage accumulation by high temperature dependent (diffusion controlled) processes [30,31] regardless the fact that $n' \neq 1$. Then, the higher the strength of the material, the lower the strain rate for a given $t_f$. Consequently, it can be inferred that a displacement of composite data on the left or on the right with respect to un-reinforced data in MG plot can be associated with two different phenomena: Data displacement on the left with respect un-reinforced alloy data is related to load transfer mechanism, whereas displacement on the right is linked to non-diffusion controlled interfacial damage phenomena.

The above trend is, in principle, also valid for the IM materials. Some questions, however, have to be raised because unexpected creep behaviors are usually found here.

This is seen, for example, in the case of AC2B-15%$Al_2O_3$ composite [26]. Its creep strength at 523 K is similar to that of the AC2B alloy, but they have very different stress exponent, *n*, (4 *vs*. 11) in the power law creep equation $\dot{\varepsilon}_{\min} = k'\sigma^n$ (where *k*' is a material's and temperature dependent constant, and $\sigma$ the stress). This is seen in the double logarithmic plot of strain rate *vs*. stress of figure 5. The consequence of the difference in *n* is that the alloy is weaker (deforms at a faster $\dot{\varepsilon}_{\min}$) than the composite in the low strain rate regime (below some $8x10^{-8}s^{-1}$), but it is stronger at a high strain rate. Also, in the composite materials of Gariboldi [27], an almost negligible effect of increasing reinforcement content on the creep strength is found, Table I. In parallel, the MG plot for these materials also presents a very similar trend, figure 2. The only cases in which $t_f$ increases with the reinforcement content are that of A359-SiCp composites of ref. [28], figure 2. Furthermore, $n'$ in these materials is extremely low (0.33 and 0.54). It should be noted, however, that the increase in creep strength of these composites is very small.

Now, it would be an interesting exercise to find a connection between these experimental observations with microstructural parameters. A microstructural parameter which has been previously correlated with MG parameters is the specific surface area [23]. This area is the sum of the grain boundary area and the matrix-reinforcement interface per unit volume. This concept is used now in the materials reviewed in Table I, and the result of the analysis conducted is summarized in the plot of Figure 6 in which the MG constant, C, is represented as a function of the specific surface area. As is shown, a similar trend is found between the analysis conducted in [23] and that resulting from this analysis when $C$ <2. For materials with C>2 (all IM materials), not reported in Figure 6, a value of the specific surface area of 0.5 is always found. When coarser microstructures are analyzed (small specific surface area), important deviations from the trend of [23] are found, as it is shown in Figure 6.

To the authors' knowledge, no other relationship between microstructural and MG parameters has been found. In summary, further work to understand the MG relationship is necessary. As mentioned above, only in the case that $n'$=1 does the phenomenological MG equation (1) have a physical meaning. A new vision of this equation is proposed here in order to deepen this understanding. Following Krasowsky and Toht [31], it can be assumed that $C = f(n')\varepsilon_f$ (where $f(n')$ is a scalar function of $n'$

(with $f(n') \leq 1$ ) and $\varepsilon_f$ is the total elongation to fracture). It is then, possible to reorganize Equation (1) to obtain,

$$t_f \, \dot{\varepsilon}_{min} \dot{\varepsilon}_{min}^{n'-1} = f(n')\varepsilon_f \tag{2}$$

When $n'$=1 it is obtained,

$$C = f(n')\varepsilon_f = \varepsilon^* \tag{3}$$

and $\varepsilon^* < \varepsilon_f$

Reorganizing equation (2) again, it is found,

$$t_f \, \dot{\varepsilon}_{min} = \frac{f(n')}{\left(\dot{\varepsilon}_{min}^{n'-1}\right)} \varepsilon_f \tag{4}$$

Now, a new attempt to find a rational interpretation of the MG relationship can be done. The left term of the equation is related to the strain accumulated during steady state creep. This is translated to the right part by diminishing $\varepsilon_f$ a factor of $\frac{f(n')}{\left(\dot{\varepsilon}_{\min}^{n'-1}\right)}$. This is an indication that, somewhat, the factor $\frac{f(n')}{\left(\dot{\varepsilon}_{\min}^{n'-1}\right)}$ quantifies the relative importance of secondary creep strain with respect to that accumulated during primary and tertiary creep stages. It should be borne in mind that it is experimentally found n′<1 for virtually all materials reported in the literature. Finally, it is worth mentioning that the new form of the equation proposed, Equation (4), resembles that of Dobeš and Milička [32] since in both cases, the elongation to failure term appears in the equation correlating $\dot{\varepsilon}_{\min}$ and $t_f$ . In future work, a more detailed discussion on this similarity and a comprehensive analysis of data from the present authors as well as data reported from the literature including this new parameter in the above correlation will be presented.

**Conclusions**

The rupture creep behavior of aluminum alloy matrix composites has been studied on the basis of results from published investigations and authors' own data. An analysis of this information has been made in the framework of the phenomenological Monkman-Grant, MG, relationship. Particular emphasis is put on the effect of the processing route

(powder metallurgy *vs.* ingot metallurgy) and reinforcement content. The following are the main conclusions of this research:

1. The MG exponent, $n'$, is always $n'<1$ in both, the composites and the un-reinforced alloys analyzed. A value of $n'=1$ is, virtually, never found. This fact adds complexity to the understanding of the MG equation and the creep rupture phenomenon on the basis of microstructural parameters and deformation mechanisms. This is because the MG constant, $C$, has a physical meaning (it can be interpreted in terms of a strain) *only* when $n'=1$.
2. In general, powder metallurgy, PM, processing leads to a smaller dispersion of the MG parameters than ingot metallurgy. This is most likely associated with a more homogeneous microstructure of these composites. In some cases, however, materials fabricated by PM lead to anomalous trends.
3. Composite data displacements on the left and on the right of the un-reinforced alloy data in MG plots are, respectively, the consequence of load transfer and damage effects associated with the reinforcement.
4. Some knowledge of the failure phenomena of metal matrix composites and alloys can be obtained by rearranging the MG equation in the following form: $t_f \dot{\varepsilon}_{min} = \frac{f(n')}{\left(\dot{\varepsilon}_{min}^{n'-1}\right)}\varepsilon_f$. The common MG equation is recovered when n′=1. The term $\frac{f(n')}{\left(\dot{\varepsilon}_{\min}^{n'-1}\right)}$ is related to the deformation on primary and/or tertiary stages (non- stationary conditions) of creep. Then, the idea that strain is the macroscopic manifestation of the damage generated and accumulated during creep would also be valid. Further work is, however, necessary to understand this term in more depth and its relation with microstructural deformation mechanisms.

**Acknowledgement**

Project MAT-05-0527 from MEC, Spain. Dr. J. Wolfenstine for providing the 6061Al-40vol%$SiC_w$ composite.

**References**


[1] T.G. Nieh, Metall. Trans. A 15 (1984) 139-145.
[2] R.S. Mishra, A.B. Pandey, Metall. Trans. A 21 (1990) 2089-2090.
[3] G. González-Doncel, O.D. Sherby, Acta Metall. Mater. 41 (1993) 2797-2805.
[4] Y. Li, T.G. Langdon, Metall. Mater. Trans. A 29 (1998) 2523-2531.
[5] K-T. Park, F.A. Mohamed, Metall. Mater. Trans. A 26 (1995)3119-3129.
[6] Z.Y. Ma, S.C. Tjong, Comp. Sci. Technol. 61 (2001) 771-786.
[7] K. Kuchařová, J. Čadek, S.J. Zhu, J. Mater. Sci. 38 (2003) 3535-3543.
[8] S. Spigarelli, M. Cabibbo, E. Evangelista, T.G. Langdon, Mater. Sci. Eng. A328 (2002) 39-47.
[9] M.F. Moreno, C.J.R. González Oliver, Mater. Sic. Eng. A418 (2006) 172-181.
[10] J.R. Pickens, T.J. Langan, R.O. England, M. Liebson, Metall. Trans. A 18 (1987) 303-312.
[11] A.F. Whitehouse, H.M.A. Winand, T.W. Clyne, Mater. Sci. Eng. A242 (1998) 57-69.
[12] R. Fernández , G. González-Doncel, Acta Mater. 56 (2008) 2549-2562.
[13] D.J. Lloyd, Int. Mater. Rev. 39 (1994) 1–23.
[14] R. Fernández R, G. González-Doncel, Scripta Mater. 59 (2008) 1135-1138.
[15] F.C. Monkman, N.J. Grant, Proc ASTM. 56 (1956) 593-605.
[16] F.R. Larson, J. Miller, Am. Soc. Mech. Eng. 74 (1952) 765-775.
[17] G.H. Edward, M.F. Ashby, Acta Mater. 27 (1979) 1505-1518.
[18] A. Needleman, J.R. Rice, Acta Mater. 28 (1980) 1315-1332.
[19] K. Davanas, A.A. Salomón, Acta Metall Mater. 38 (1990) 1905-1916.
[20] M.W. Decker, J.R. Groza, J.C. Gibeling, Mater. Sic. Eng. A369 (2004) 101-111.
[21] K.M.B. Taminger, Master´s Thesis. 1999. Available inhttp://scholar.lib.vt.edu/theses/available/etd-030299-114237/
[22] A.B. Pandey, R.S. Mishra, Y.R. Mahajan, J. Mater. Sci. 28 (1993) 2934-2949.
[23] D.C. Dunand, B.Q Han, A.M. Jansen, Metall. Mater. Trans. 30A (1999) 829-838.
[24] K. Ishikawa, Y. Kobayashi, Mater. Sci. Eng. A 387-389 (2004) 613-617.
[25] Z.Y. Ma, S. C. Tjong, S. X. Li, J. Mater. Res. 14 (1999). 4541-4550.
[26] H.W. Nam, K.S. Han, Metall. Mater. Trans. A. 29A (1998). 1983-1989.
[27] E. Gariboldi, M. Vedani, Int. J. Mater. Prod. Technol. 17 3/4 (2002) 243-260.
[28] N.P. Hung, C.S. Lim, Y.K. Ho, Y.C. Tan, W.G. Tan, J. Mat. Proc. Tech. 101 (2000) 104-109.
[29] A. F. Whitehouse, H. M. A. Winand, T. W. Clyne, Mater. Sci. Eng. A242 (1998) 57-69.
[30] R. Raj, M.F. Ashby, Acta Metall. 23 (1975) 653-666.
[31] A.J. Krasowsky, L. Toht, Metall. Mater. Trans. A 28 (1995) 1831-1842.
[32] F. Dobeš, K. Milička, Metal Sci. 10 (1976) 382-384.

| Authors [ref.] | Material | Processing | Stress, MPa | Temp, K | MG exponent $n'$ | MG constant, $C$ | Improved composite creep behavior † | Microstructure |
|---|---|---|---|---|---|---|---|---|
| **Fernández, González-Doncel [14]** | 6061Al<br>6061Al-15vol%$SiC_w$ | PM | 11 - 40<br>5 - 49 | 573- 723<br>623- 773 | 0.80<br>0.67 | 0.90<br>1.16 | (+) | Extruded. Grain size (3.5 μm and 1.5μm for composite). Low aspect ratio and size 0.4*0.8 $\mu m^2$ |
| **Monkman, Grant [15]** | Al, 2S,3S and Zn, Mg and Cu Solid solutions of Al. | IM | - | 288- 593 | 0.85 | 1.3 | | |
| **Taminger *et al.* [21]** | 2124Al<br>2124Al-15% $Al_2O_3w$ | PM | 76 - 271<br>59 - 256 | 394- 539<br>367- 541 | 0.73<br>0.91 | 1.40<br>0.48 | (-) | Grain size (250 μm and 77μm for composite) Size0.5*10 $\mu m^2$ |
| **Pandey *et al.* [22]** | Al-10%SiCp<br>Al-20%SiCp<br>Al-30%SiCp | PM | 24.5 – 30.5<br>36.0– 44.0<br>48.5 – 54.0 | 623 | 0.74<br>0.77<br>0.85 | 0.85<br>0.16<br>0.04 | (+)†† | SiCp particle size 1.7μm. |
| **Dunand *et al.* [23]** | Al99,9%-25%$Al_2O_3$p Corase Grain (CG)<br>Al99,9%-25%$Al_2O_3$p Fine Grain (FG) | IM<br>PM | 30 – 100 | 608- 723 | 0.84<br>0.93 | 0.133<br>0.05 | PM material stronger than IM | Grain size 1.3μm. Particles of 0.28 μm |
| **Ishikawa *et al.* [24]** | 5083Al | IM | - | 623- 773 | 0.83 | 0.606 | | Grain size 100 μm. |
| **Ma *et al.* [25]** | Al-$TiB_2$p | Reactive hot press. (Not PM) | 28 – 118 | 573-673 | 0.91 | 0.04 | | Extruded fully dens. Particles of around 1μm |
| **Nam, Han [26]** | AC2B (Al-Fe-V-Si-Mn)<br>AC2B-15%$Al_2O_3$ fibers | Squeeze cast (Not PM) | 84 – 147<br>86 – 151 | 523 | 1.00<br>0.55 | 0.002<br>5.97 | (+) or (-) depending on strain rate. See fig. 5. | Reinforcement size 3x60 $\mu m^2$. |
| **Gariboldi *et al.* [27]** | 6061Al-10vol% $Al_2O_3$p<br>6061Al-20vol% $Al_2O_3$p | IM | 50 – 300 | 423- 523 | 0.40<br>0.69 | 263.98<br>3.20 | Similar creep strength of 10vol% and 20vol% composites | Grain size 7 μm. Particle size 9.9 μm for 10% and 20.6 for 20%. |
| **Hung *et al.* [28]** | A359<br>A359-10%SiCp<br>A359-20%SiCp | IM | 50-146 | 448- 573 | 0.42<br>0.54<br>0.33 | 283.45<br>179.28<br>3531.9 | (+) | Not fully dens. Voids presence Reinforcement around 10 μm |
| **Whitehouse *et al.* [29]** | Pure aluminum unreinforced<br>-10% safil powder<br>-10% safil infiltr.<br>-10% carbon<br>-10% whiskers | PM | 20 – 46<br>25 – 40<br>20 – 30<br>25 – 40<br>50 – 60 | 543 | 0.60<br>0.68<br>0.98<br>0.76<br>0.91 | 362.09<br>1.19<br>0.07<br>0.90<br>0.05 | (+) | Reinforcement size in the range of 5 – 13 μm |
| **Present research** | 6061Al-40vol% $SiC_w$ | PM | 23.0 – 73.0 | 673- 723 | 0.77 | 0.16 | (+) | |

† Symbol (+) refers to an increase of the composite creep behavior with respect to the un-reinforced alloy. Symbol (-) indicates that composite is weaker than the alloy.
†† No comparison with un-reinforced alloy, but composite creep strength increases with % of reinforcement content.

Table I. Summary of the creep failure studies in the literature on discontinuously reinforced aluminium alloy matrix composites MMCs (some of them include data of the corresponding un-reinforced alloys) and monolithic aluminium alloys.

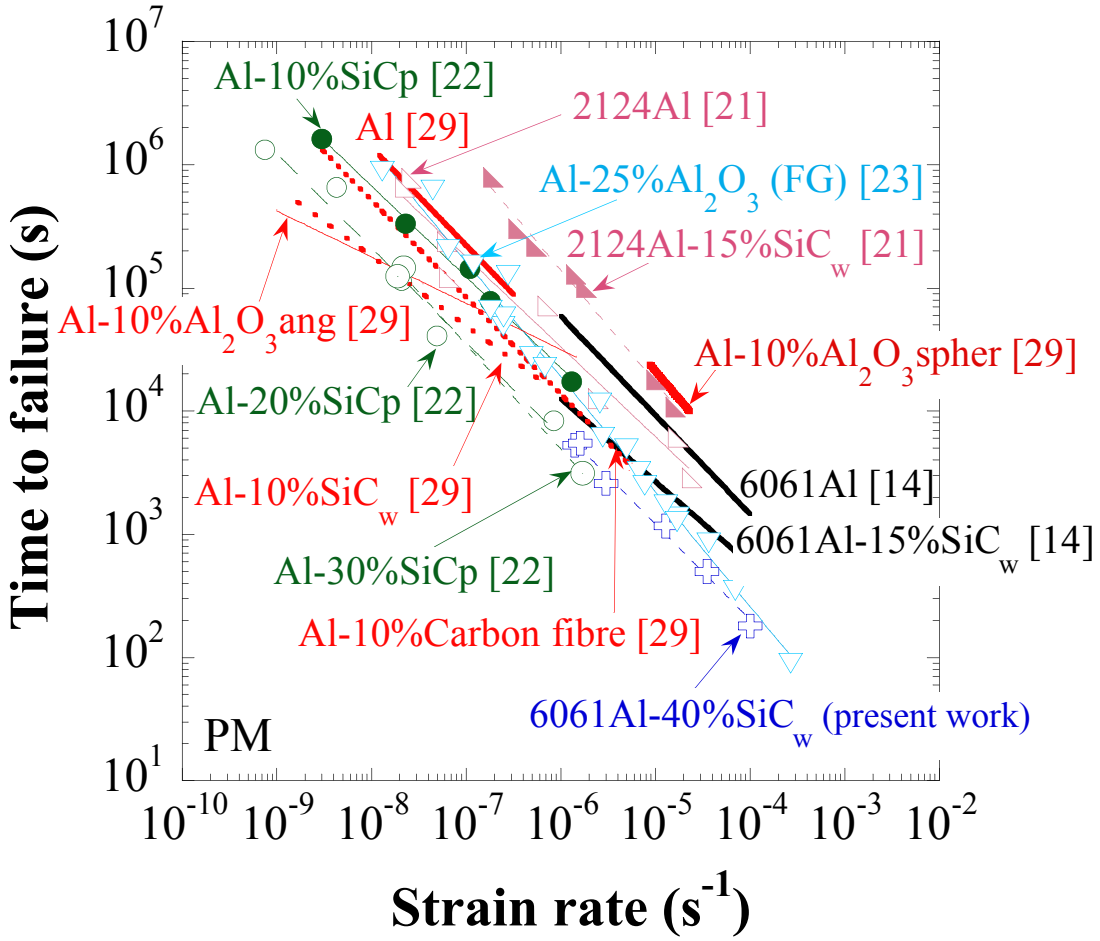


Figure 1. Monkman-Grant plot for the data of the PM materials analyzed. Number in brackets in each material indicates reference from the list of references. FG on Al-25%$Al_2O_3$ composite of ref. [23] indicates fine grains.

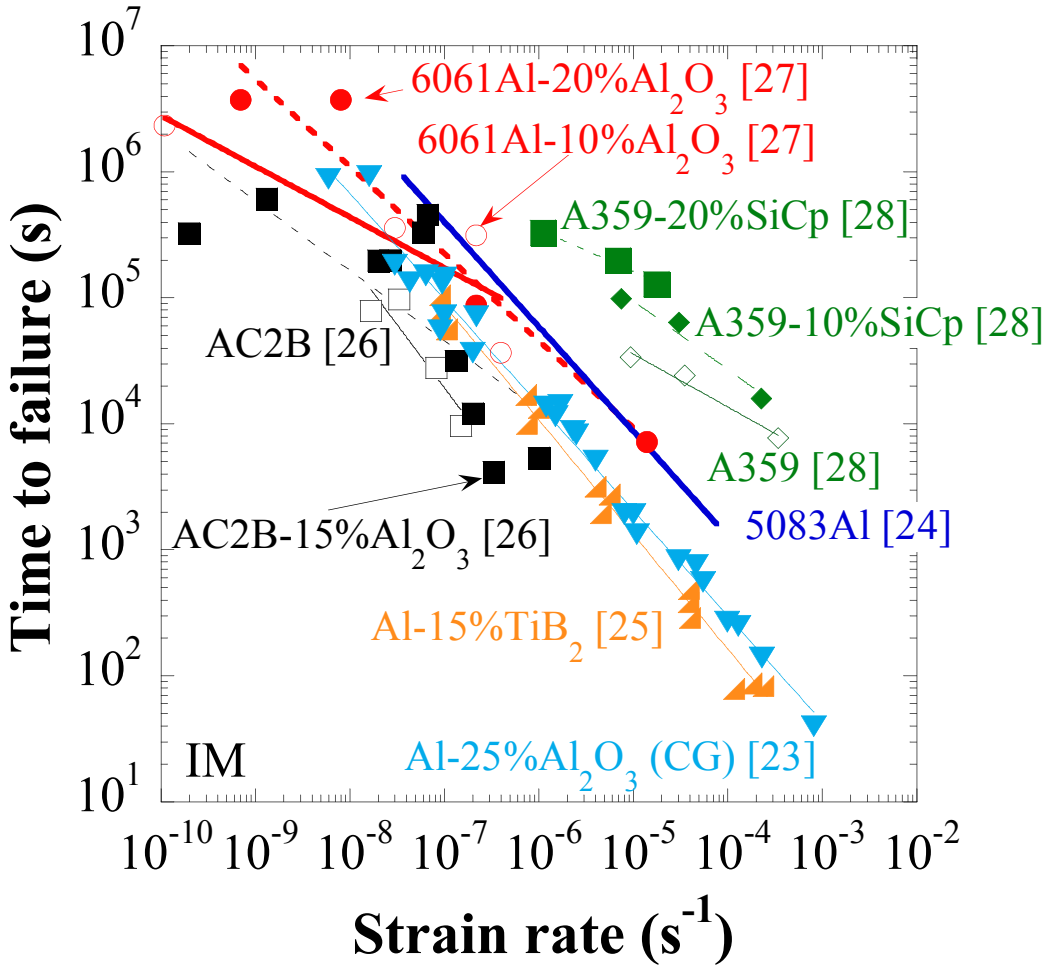


Figure 2.- Monkman-Grant plot for materials processed by IM and other routes different from PM. Number in brackets in each material indicates reference from the list of references. CG on Al-25%$Al_2O_3$ composite of ref. [23] indicates coarse grains. In the case of 5083Al alloy of ref. [24], only the data fit is presented for clarity.

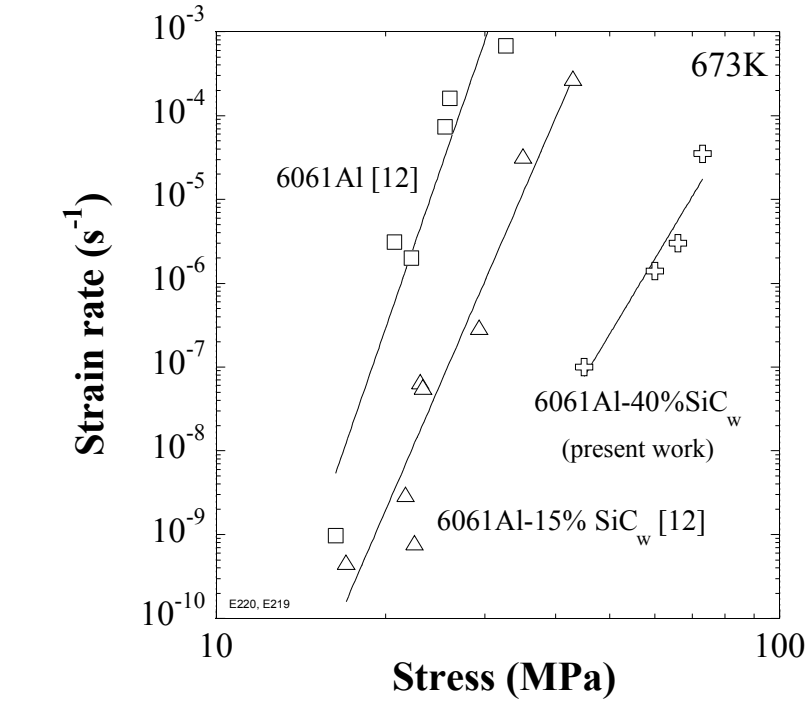


a)

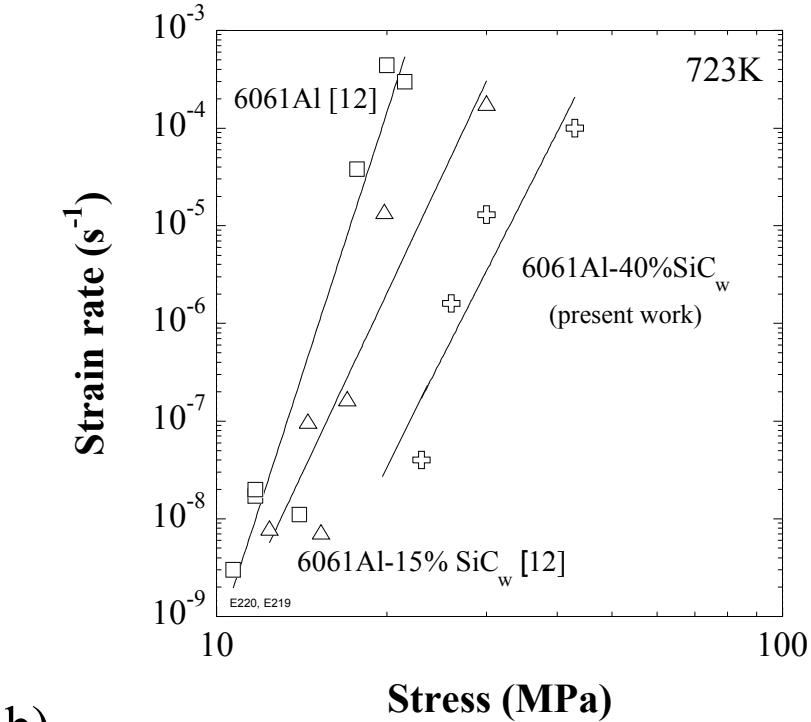


b)

Figure 3. Double logarithmic plot of strain rate *vs*. stress of the PM 6061Al-40vol%$SiC_w$ composite in comparison to the behavior of the 6061Al-15vol%$SiC_w$ composite and 6061Al alloy investigated in [12]. a) at 673 K, b) at 723K. The improved creep response with increasing reinforcement content is evident.

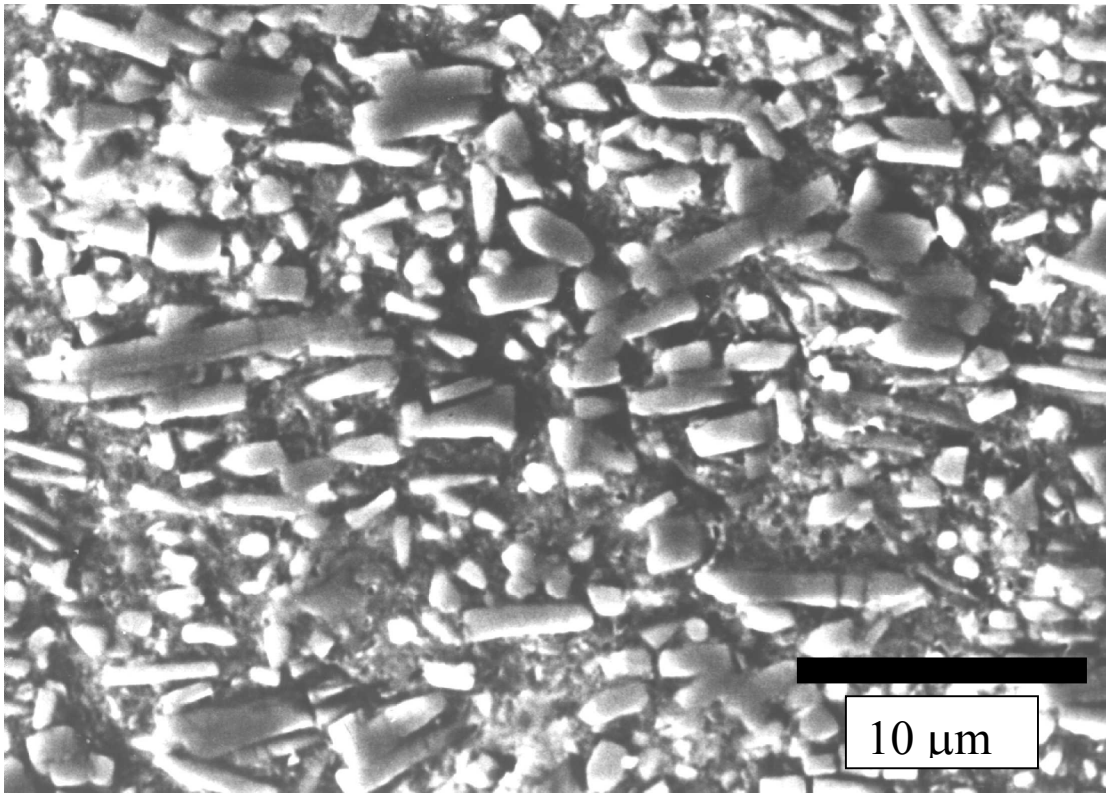


Figure 4.- Microstructure of the 6061Al-40vol%$SiC_w$ composite. The extrusion direction is the horizontal one.

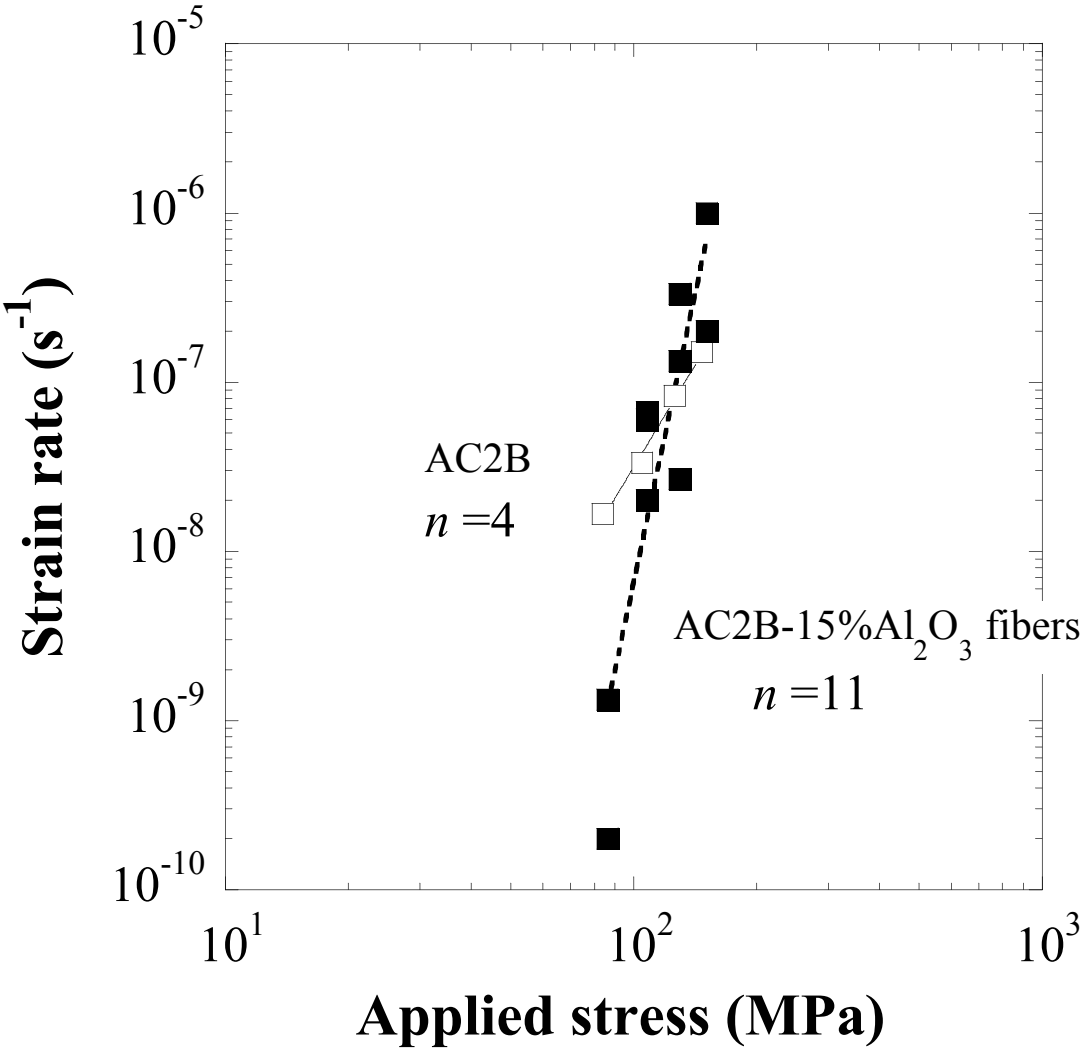


Figure 5.- Double logarithmic plot of strain rate *vs*. stress of the AC2B alloy and AC2B-15vol%$Al_2O_3$ fibers composite investigated in [26], Table I. The stress exponent is $n$=4 in the alloy and $n$=11 in the composite. The composite is stronger than the alloy at low stress and weaker at high stress.

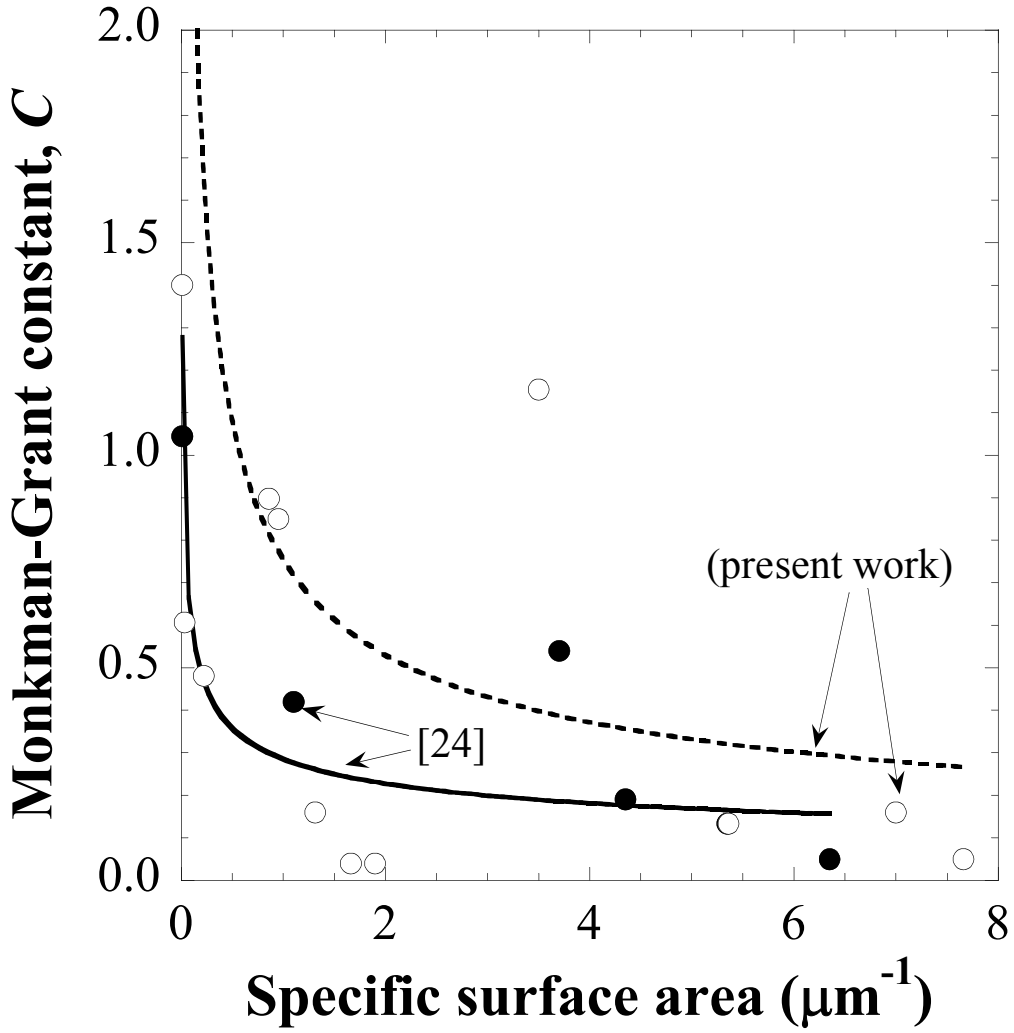


Figure 6.- Variation of the Monkman-Grant constant, *C*, with the specific surface area in the analysis conducted in [23] and the present work when $C<2$. As can be seen, a similar trend (continuous and dotted line, respectively) is observed in both cases.

**Figure captions**

Figure 1. Monkman-Grant plot for the data of the PM materials analyzed. Number in brackets in each material indicates reference from the list of references. FG on Al-25%$Al_2O_3$ composite of ref. [23] indicates fine grains.

Figure 2.- Monkman-Grant plot for materials processed by IM and other routes different from PM. Number in brackets in each material indicates reference from the list of references. CG on Al-25%$Al_2O_3$ composite of ref. [23] indicates coarse grains. In the case of 5083Al alloy of ref. [24], only the data fit is presented for clarity.

Figure 3. Double logarithmic plot of strain rate *vs*. stress of the PM 6061Al-40vol%$SiC_w$ composite in comparison to the behavior of the 6061Al-15vol%$SiC_w$ composite and 6061Al alloy investigated in [12]. a) at 673 K, b) at 723K. The improved creep response with increasing reinforcement content is evident.

Figure 4.- Microstructure of the 6061Al-40vol%$SiC_w$ composite. The extrusion direction is the horizontal one.

Figure 5.- Double logarithmic plot of strain rate *vs*. stress of the AC2B alloy and AC2B-15vol%$Al_2O_3$ fibers composite investigated in [26], Table I. The stress exponent is $n$=4 in the alloy and $n$=11 in the composite. The composite is stronger than the alloy at low stress and weaker at high stress.

Figure 6.- Variation of the Monkman-Grant constant, $C$, with the specific surface area in the analysis conducted in [23] and the present work when $C$<2. As can be seen, a similar trend (continuous and dotted line, respectively) is observed in both cases.